

An electrochemical sensing platform for sensitive detection DNA methylation using Fe₃O₄/TMC/Au nanocomposite and poly(L-arginine)/reduced graphene oxide modified screen-printed carbon electrode

Leila Syedmoradi,^a Hassan Hajghassem,^b Gholamreza Tavoosidana,^c Seyed Mahdi Rezayat,^a Reza Faridi-Majidi,^{a*} and Kobra Omidfar^{d,e*}

^aDepartment of Medical Nanotechnology, School of Advanced Technologies in Medicine, Tehran University of Medical Sciences, Tehran, Iran.

^bDepartment of Microelectromechanical systems, Faculty of New Sciences and Technologies, University of Tehran, Tehran, Iran.

^cDepartment of Molecular Medicine, School of Advanced Technologies in Medicine, Tehran University of Medical Sciences, Tehran, Iran.

^dBiosensor Research Center, Endocrinology and Metabolism Molecular-Cellular Sciences Institute, Tehran University of Medical Sciences, Tehran, Iran.

^eEndocrinology and Metabolism Research Center, Endocrinology and Metabolism Research Institute, Tehran University of Medical Sciences, Tehran, Iran.

Correspondence to Reza Faridi-Majidi and Kobra Omidfar (email: refaridi@sina.tums.ac.ir, omidfar@tums.ac.ir).

(Submitted: 16 July 2018 – Revised version received: XX XXXX XXXX – Accepted: XX XXXX XXXX – Published online: XX XXXX XXXX)

Objective This study, a simple electrochemical nanosensor has been developed for the rapid and sensitive detection of methylated Septin 9 DNA as a useful biomarker for early colorectal cancer detection or screening.

Methods The process consists of three main steps: (i) The surface modification of screen-printed carbon electrode (SPCEs) with a poly(L-Arg)/reduced graphene oxide composite film followed by immobilizing anti-5-methylcytosine antibody, (ii) preparation of probe-modified Fe₃O₄/N-trimethylchitosan/Au nanocomposites for the hybridization with complementary DNA sequences, (iii) capturing methylated DNA target by antibody-modified SPCEs and subsequent electrochemical detection through redox peak currents of gold nanoparticles which generated a concentration-dependent response.

Results The surface modification of the electrode and hybridization with the methylated target were confirmed by cyclic voltammetry method and differential pulse voltammetry was used for quantitative evaluation of methylated target DNA.

Conclusion The assay showed a wide linear range from 0.01 to 1000 pM with a low detection limit of 0.01 pM.

Keywords Fe₃O₄/TMC/Au nanoparticle, polyarginine, DNA methylation, SEPT9, anti-5-methylcytosine antibody

Introduction

DNA methylation, best-known epigenetic modifications, provides a useful source of biomarkers for cancer classification and prognosis.^{1,2} The first evidence on link between DNA methylation and cancer was reported by Feinberg and Vogelstein³ and afterward, the analysis of DNA methylation biomarkers, has become one of the attractive field in early cancer diagnosis, prognosis and therapeutic monitoring.^{4,5}

To date, the huge number of DNA methylation biomarkers have been discovered and analyzed in various malignancies including prostate cancer, breast cancer, lung and colorectal cancers.^{5,6}

Methylated Septin 9 (mSEPT9) DNA has been reported as a biomarker for screening and early detection of colorectal cancer (CRC).^{7,8} A number of clinical trials have evaluated the performance of mSEPT9 in human plasma for CRC detection. The sensitivity and specificity of mSEPT9 in these studies varied from 50–90% to 88–91%, respectively, depending on the experimental assays.^{7–9}

Up to now, several methods have been developed to detect methylated DNA biomarkers including methylation-specific Polymerase chain reaction (PCR). (MS-PCR), pyrosequencing, bisulfate sequencing, methylation specific microarray and methylation-specific fluorescence resonant energy transfer.^{10,11}

However, these methods are complicated and time-consuming, requiring a large amount of purified PCR samples and costly instrumentation which limit the use of them in clinical laboratories. During the past decade, the different models of biosensor technologies including electrochemical, electrical, optical, and mass based methods have been

developed and reported for the detection of methylated DNA allowing rapid, easier to use and cost effective diagnostic than conventional methods.^{12,13}

Among these biosensors, electrochemical biosensors have been widely applied in biosensing due to their unique features such as high sensitivity, rapid and simple implementation, low cost, and compatibility with miniaturization technologies.^{14,15} Furthermore, the incorporation of nanomaterials and conductive polymers into electrochemical biosensors can efficiently improve the assay sensitivity as well as enhance signal-to-background ratio and stability of biosensors.^{16,17}

In this study, SPCEs modified with reduced graphene oxide (RGO) and poly(L-arginine) [poly(L-Arg)] was used as sensing platform. Graphene oxide (GO) and RGO show great potential for electrochemical biosensing due to their large surface area, good electrical properties, ease of synthesis and functionalization, good water dispersity, and excellent biocompatibility. These properties make graphene-based nanomaterials excellent scaffolds for the construction of sensitive electrochemical biosensors for a variety of analytes.^{18–20} Recent research reported the electrodes covered with RGO showed better electrochemical biosensing performance as compared to bare electrode or electrodes modified with carbon nanotubes.²¹

Electrochemical reduction is commonly used for the subsequent reduction of predeposition GO to RGO on electrode surface due to its simplicity, fast, low-cost, and greater efficiency rather than other approaches such as chemical and thermal reduction.^{21–23}

In addition to graphene based nanomaterials, poly(amino acid)-modified electrodes such as poly(L-Arg) have also been used in electrochemical sensing due to their excellent electrocatalytic ability. Poly(L-Arg) possesses a protein-like structure containing a positively guanidyl group which able to interact with the negatively charged groups of GO through electrostatic interactions.^{24,25} Thus, the poly(L-Arg)/RGO composite film can take advantage of the good electronic properties of graphene and excellent electrocatalytic activity of L-arginine, leading to the excellent performance of sensing platform.^{24,26}

Here, we report an immuno-DNA based technique for the simple and fast detection of SEPT9 methylated DNA target, considered a useful biomarker for screening and early detection of CRC. In this work, RGO-modified SPCEs were prepared by the electrochemical reduction of GO suspension predeposited on electrode surfaces. The RGO-modified electrodes were then coated with the poly(L-Arg), followed by the simple entrapment of anti-5-methylcytosine (anti-5mC) antibody on the polymer-modified surfaces. Next, Fe₃O₄/N-trimethylchitosan (TMC)/Au nanocomposites modified with biotinylated Single-strand DNA (ssDNA) probe are used for the subsequent hybridization between DNA target sequence and nanoparticle-DNA probes. Finally, the nanoprobe-DNA hybrid was captured by the antibody-modified SPCEs, which in turn produce a signal current proportional to the amount of DNA target.

Experimental Section

Materials and Reagents

Chemicals

Ferric chloride hexahydrate (FeCl₃·6H₂O), ferrous chloride tetrahydrate (FeCl₂·4H₂O), NaOH, and acetic acid were obtained from Acros Organics (USA). Chloroauric acid (HAuCl₄), sodium dodecyl sulfate (SDS), low molecular weight chitosan, dialysis tube with molecular cutoff 12,000 Da, sodium azide, streptavidin, monoclonal anti-5mC antibody, GO and L-arginine were purchased from Sigma Chemical Company (St. Louis, MO, USA). The analytical HCl, NaCl, D-glucose, glutaraldehyde, N-methyl pyrrolidone (NMP), iodomethane, sodium hydroxide, sodium iodide and acetone were purchased from Merck (Darmstadt, Germany). All other chemicals used were of analytical grade and deionized water was used in all the experiments. The SPCEs (3.4 cm length × 1.0 cm width × 0.05 cm height) were purchased from DropSens (Spain).

Oligonucleotides

Biotinylated ssDNA probes and target methylated DNA sequences used in this study were purchased from Tag Copenhagen A/S (Denmark); the DNA sequences are listed as follows:

Methylated sequence (target):

5' - mCGGmCGCCCCAGCCAGmCGmCGCAGGGC
CmCGGGCCmCGmCGGGGGmCGC-3'

Probe sequence:

5'-GGCCCGGGCCCTGCGCGCTG-biotin-3'

Procedures

Preparation of Au/TMC/Fe₃O₄ Nanocomposites

The Au/TMC/Fe₃O₄ nanocomposites is composed of three layers (magnetic core, intermediate TMC polymer, and gold

NPs coating shell) were separately prepared according to the previous literature. Briefly, Fe(II) and Fe(III) chloride were dissolved in distilled water at a ratio of 0.5 and Fe₃O₄ nanoparticles were then precipitated in the presence of NaOH.²⁷

The TMC polymer was prepared using iodomethane in the presence of NMP and NaOH according to previous publication. Colloidal Au nanoparticles were synthesized by the reduction of aqueous HAuCl₄ with D-glucose in the presence of NaOH at 60°C.

In the following, a thin layer of previously produced TMC polymer was coated on Magnetic nanoparticle (MNP). by use of the cross-linker glutaraldehyde. For this purpose, the 1:1M ratio of Fe₃O₄ to TMC, were dissolved in a solution containing glutaraldehyde, NaCl, and SDS. The mixture was incubated at 50°C for 5 h under stirring to obtain TMC coated nanoparticles. Next, 200 mg of TMC@Fe₃O₄ NPs were exposed to 25 mL of colloidal gold NPs at room temperature for 1 h under stirring condition. The product, Fe₃O₄/TMC/Au nanocomposites, was magnetically pelleted, washed with PBS and kept away from light at 4°C after adding sodium azide (0.01%).^{27,28}

Characterization of Produced Nanomaterials

The size and morphology of Fe₃O₄ nanoparticles, Fe₃O₄/TMC nanocomplexes, and Au/TMC/Fe₃O₄ were evaluated by transmission electron microscopy (TEM) (Zeiss, EM10C, 80 kV, Germany). The chemical interactions in the product formulation was confirmed by Fourier transform infrared spectroscopy (FTIR).

In addition to above-mentioned characterization, the crystallinity of the nanocomposites and magnetic properties of magnetic nanomaterials were studied by X-ray diffraction and vibrating sample magnetometer respectively as previously reported by our group.^{16,29}

Preparation of Nanocomposite-conjugated Probes

The biotin-labeled probe was attached onto the Au/Fe₃O₄ NPs through a two steps process: (1) Coating the Au/Fe₃O₄ NPs with streptavidin; (2) immobilization of biotinylated DNA probe onto the streptavidin-coated NPs. First, to prepare the streptavidin-coated NPs, 20 µg streptavidin dissolved in 500 µL PBS was added to the 20 mg of Au/TMC/Fe₃O₄ NPs and incubated at 37°C for 1 h under shaking condition. The streptavidin was electrostatically conjugated with the gold magnetic particles. The nanocomposites were washed and magnetically separated. The products were then magnetically separated and washed. The coupling efficacy was then evaluated by measuring the OD₂₈₀ values of streptavidin suspension before and after conjugation process. Next, the biotinylated ssDNA probe which could specifically detect SEPT9 was immobilized onto the streptavidin-coated NPs. 250 microliters of PBS buffer containing 400 pmol of biotinylated DNA probe was added to streptavidin-coated nanocomposites and incubated at 37°C under shaking condition.

Finally, the particles were rinsed with PBS buffer and the immobilization efficiency was estimated from the OD₂₆₀ values of the oligonucleotide solutions pre- and post-immobilization process.

Fabrication of Poly(L-Arg)/RGO-Modified Electrode

The SPCEs consist of a carbon working electrode (4 mm diameter), carbon counter electrode, and a silver pseudo-reference electrode. First, 5 µL of 1 mg ml⁻¹ GO in water was

drop-casted onto the working electrode and a thin film of RGO was formed by CV method from -1.5 to 0 V vs. Ag/AgCl for 10 cycles at a scan rate of 100 mV s^{-1} .^{22,30} The modified electrode was then washed with PBS solution to remove remaining GO particles on the electrode surface.

Next, $50 \mu\text{L}$ of L-Arg was electrodeposited onto RGO-modified SPCE surface by CV method from -2 to 2 V at 100 mV s^{-1} for seven cycles.^{24,25} After a washing step, $5 \mu\text{L}$ of PBS solution containing 100 ng of anti-5mC antibody was added to the working zone of each SPCE and kept overnight at 4°C . The Ab-modified SPCEs were washed with PBS buffer to remove the excess Ab and unreacted surface sites were then blocked using BSA (3%) for 15 min.

Quantification of Methylated DNA by using Fabricated Nanobiosensor

Hybridization process

The hybridization was performed by stirring at room temperature. First, various concentrations of methylated DNA target were prepared in PBS buffer and then, 4 mg of probe-modified NPs was added to each concentration and incubated for 2 h under gently shaking.

After hybridization process, the NPs were magnetically separated, washed, and re-suspended in PBS buffer. In the following, $20 \mu\text{L}$ of the resulting suspensions were added to the Ab-modified SPCEs and kept at 37°C for 40 min under gently shaking. After a washing step with PBS, the electrodes were assessed by electrochemical measurements.¹⁶

Electrochemical measurements:

Electrochemical characteristics of stepwise modifies electrodes were performed CV mode and differential pulse voltammetry (DPV) method using $50 \mu\text{L}$ of HCl (1M) on the surface of modified electrodes.

All electrochemical measurements, performed at room temperature, involved oxidoreduction of gold nanoparticles in the nano-complex. The basic analysis of the SPCEs was obtained through CV mode, at the potential range of -0.7 to $+1.1$ V and the scan rate of 50 mV s^{-1} . The performance of the biosensor was evaluated by DPV mode.^{16,28}

The specificity of the constructed biosensor was evaluated by using the PCR-amplified unmethylated DNA sequence as a negative control in this sensing platform.

The accelerated stability of the modified electrodes was assessed every 7 h for over 3 days at 37°C , and was compared with newly prepared electrodes. Furthermore, the reproducibility of assay was evaluated using detection of two concentrations in independent measurements.³¹

RESULTS AND DISCUSSION

Strategy of Analysis

The goal of this study was to define the valuable properties of nanomaterial and conductive polymer for development of an ultrasensitive DNA-based electrochemical nanobiosensor. In this work, poly(L-Arg)/RGO composite film and $\text{Fe}_3\text{O}_4/\text{TMC}/\text{Au}$ nanocomposite were applied to make a highly sensitive assay that can detect DNA methylation. To increase the sensitivity of the assay, $\text{Fe}_3\text{O}_4/\text{TMC}/\text{Au}$ nanocomposite was used as a tracing tag to label DNA probe.³² Besides, the composite film made of conducting RGO/Arg was electrochemically polymerized on the SPCEs. $\text{Fe}_3\text{O}_4/\text{TMC}/\text{Au}$ nanocomposite-labeled DNA probe was used to capture the target sequence, and then on RGO/Arg/anti-5mC modifies SPCE recognition was performed between methylated DNA and anti-5mC antibody. An overview of the detection process is proposed in Fig. 1.

Characterization of $\text{Fe}_3\text{O}_4/\text{TMC}/\text{Au}$ Nanoparticles

Transmission electron microscopy was used to investigate the size and shape of the Fe_3O_4 , $\text{Fe}_3\text{O}_4/\text{TMC}$ and $\text{Fe}_3\text{O}_4/\text{TMC}/\text{Au}$ nanoparticles. The monodisperse Fe_3O_4 nanoparticles with a diameter of about 10 nm can be seen in Fig. 2a. A core-shell structures with a diameter of 12 nm was observed for the magnetic $\text{Fe}_3\text{O}_4/\text{TMC}$ nanocomposite (Fig. 2b). After the assembly of gold NPs on the surface of $\text{Fe}_3\text{O}_4/\text{TMC}$ nanocomposite, the diameter of the final nanocomposites has significantly enhanced and reached 20 nm (Fig. 2c). FTIR analysis was used in order to study the positive assembly of TMC-coated Fe_3O_4 NPs and final $\text{Fe}_3\text{O}_4/\text{TMC}/\text{Au}$ nanocomposites. As seen in Fig. 3, in FTIR spectra of TMC four typical peaks were observed at about 3430 cm^{-1} (overlap of O-H and intermolecular hydrogen bonding vibrations), 2900 cm^{-1} (assign to the C-H bond), 1650 cm^{-1} (ascribe the N-H bending vibration) and 1070 cm^{-1} (C-O-C stretching vibration). Furthermore, two specific peaks at about 1470 and 1600 cm^{-1} can be used for differentiating TMC from chitosan. In FTIR spectra of $\text{Fe}_3\text{O}_4/\text{TMC}$

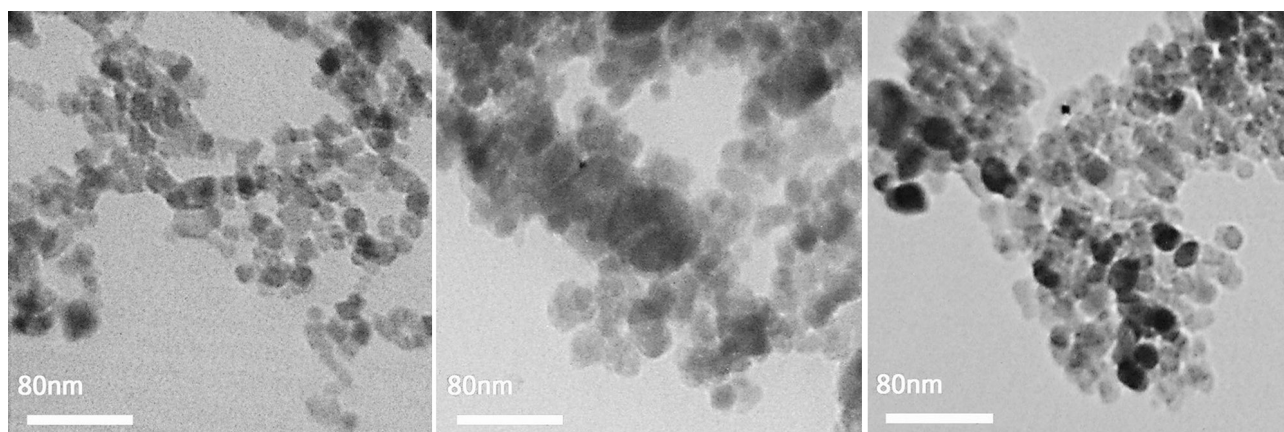


Fig. 1 Schematic of the principal mechanism for methylated DNA detection by the genosensor.

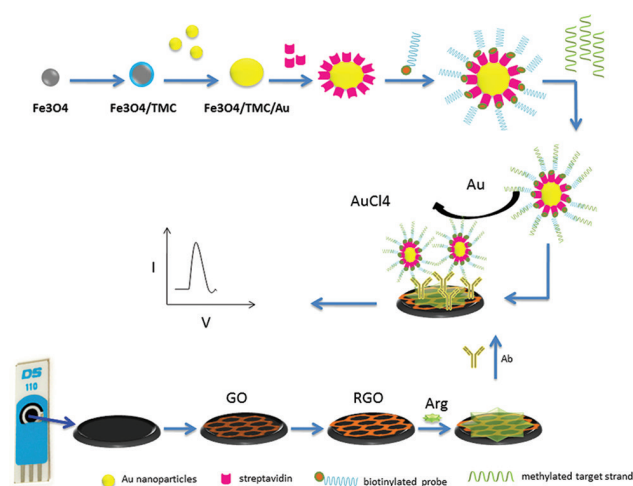


Fig. 2 TEM images of the Fe_3O_4 (a), $\text{Fe}_3\text{O}_4/\text{TMC}$ (b) and $\text{Fe}_3\text{O}_4/\text{TMC}/\text{Au}$ (c) nanoparticles.

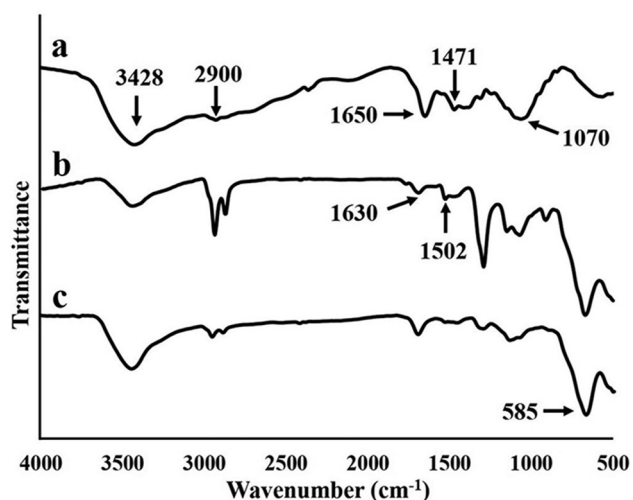


Fig. 3 FTIR spectra of TMC (a), $\text{Fe}_3\text{O}_4/\text{TMC}$ (b) and $\text{Fe}_3\text{O}_4/\text{TMC}/\text{Au}$ (c) nanoparticles.

nanocomposite we found a detectable peak at about 1502 cm^{-1} that can relate to the shifted N–H bond. There is an additional peak at about 1630 cm^{-1} which was made due to the interaction between the N–H groups of the TMC and the CHO group of glutaraldehyde. Lastly, a strong peak at about 585 cm^{-1} (curves b and c) is assigned to the Fe–O bonds and obtained from naked Fe_3O_4 particles.^{16,27}

Characterization of Streptavidin Coupled $\text{Fe}_3\text{O}_4/\text{TMC}/\text{Au}$ Nanocomposite

Streptavidin was immobilized on the surface of Au nanoparticle in $\text{Fe}_3\text{O}_4/\text{TMC}/\text{Au}$ nanostructure by physical adsorption. UV spectroscopy analysis of the reaction solution, both before and after immobilization of streptavidin was applied to evaluate the amount of streptavidin conjugated onto the surface of $\text{Fe}_3\text{O}_4/\text{TMC}/\text{Au}$ nanocomposite. The freshly prepared streptavidin solution before coupling demonstrates a maximum absorption at 280 nm. The OD_{280} values of pre- and post-immobilization defined the efficiency of 83% for the binding of streptavidin to the whole nanocomposite.

Immobilization of Biotinylated DNA Probe Onto the Streptavidin $\text{Fe}_3\text{O}_4/\text{TMC}/\text{Au}$ Nanocomposite

Streptavidin– $\text{Fe}_3\text{O}_4/\text{TMC}/\text{Au}$ particles was bound to the biotin labeled probe through the interaction between streptavidin and biotin. The non-covalent interaction between streptavidin and biotin is exceptionally fast and consistent. $\text{Fe}_3\text{O}_4/\text{TMC}/\text{Au}$ nanocomposite was not only used as a label in this study, but also applied as the immobilization substrate and separation system that is actually essential in biosensors development. We detected an immobilization efficacy of about 87% by measuring the OD_{260} values before and after immobilization.

Characterizations of Poly(L-Arg)/RGO Composite Film

The surface modification of the SPCEs with poly(L-Arg)/RGO composite film were assessed with electrochemical characterization. The surface of bare SPCEs were coated with a thin layer of RGO through electro-deposition of GO solution. A cathodic peak appeared at -0.8 V which is attributed to the chemical reduction of the oxygen-containing groups in GO. Meanwhile, the cathodic peak slightly shifted toward a more positive potential and the peak current decreased with each cycle (data not shown). This results confirm depositing GO and its reduction to RGO on the SPCE surface.

The second step of electrode modification was performed by the polymerization of L-Arg, the potential was cycled between -0.2 and $+2\text{ V}$ vs. SPCE. Resulted voltammogram of poly(L-Arg)/RGO/SPCE shows the current peak of arginine increased with CV scan rates indicating that arginine was electropolymerized on the SPCE surface (data not shown).

Electrochemical Characterization of the Genosensor

To confirm the accuracy of the genosensor preparation procedure, each step of surface modification was investigated using CV. Figure 4 presents the CV obtained at bare SPCE, RGO-modified SPCE, Arg-modified SPCE and RGO/Arg-modified SPCE in the presence of $5.0\text{ mM } [\text{Fe}(\text{CN})_6]^{3-/4-}$ containing 0.1 M KCl .

Comparing with the bare SPCE, redox peak currents were obviously increased with the formed layers, demonstrating electrical conductivity of the composite film is good which in

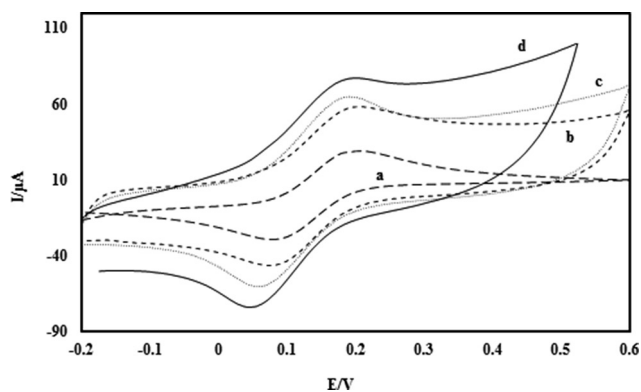


Fig. 4. Cyclic voltammograms of the modified electrodes in $5.0\text{ mM } [\text{Fe}(\text{CN})_6]^{3-/4-}$ containing 0.1 M KCl after each step of modification: bare electrode (a), RGO-modified electrode (b), Arg-modified electrode (c), RGO/Arg-modified electrode (d).

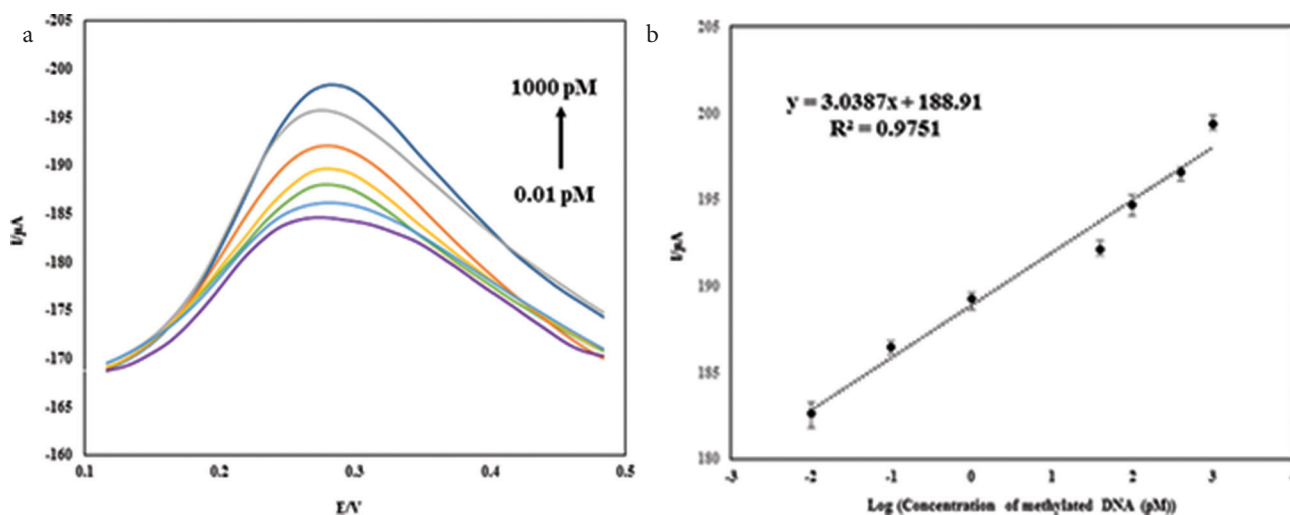


Fig 5. (a) Differential pulse voltammograms for the electrochemical detection of methylation upon serial dilutions of target between 0.01 and 1000 pM in 1M HCl. The concentrations of target methylated DNA are: 0.01, 0.1, 1, 10, 100, 500, and 1000 pM. (b): The calibration curve of methylated DNA as the relationship between current and methylated DNA concentration. Each data point is the average of three replicates.

Table 1. Spike and recovery results obtained from methylation-nanobiosensor in plasma. Data are presented as the means of three replicates

Added methylated DNA (pM)	Detected methylated DNA (pM)	Recovery (%)	RSD%
10	10.43 ± 0.6	104.3	5.25
100	101.67 ± 2.32	101.67	2.03
1000	998.10 ± 6.17	99.84	0.63

turn lead to the enhancement of electron transfer between the surface of the composite layer and the electrode.

Analytical Performance for Quantitative Detection of Methylated DNA

The quantitative analysis of methylated DNA target was investigated by DPV because this method can provide high current sensitivity and peak resolution. The standard solutions with concentration ranging from 0.01 to 1000 pM methylated DNA target were prepared by diluting the stock solution with PBS. Analyses were performed in triplicates for each concentration.

Differential pulse voltammetry measurements were performed between +0.05 and +0.35 V at scan rate of 50 mV/s by holding the working electrode at a condition potential of +1.3 V for 70 s in HCl.

As shown in Fig. 5a, the reduction peak current of gold nanoparticles gradually enhanced with increasing the concentration of methylated DNA from 0.01 to 1000 pM. The increased values of current for methylated DNA concentration are shown in Fig. 5b. The limit of detection of this method was calculated to be 0.01 pM.

Reproducibility and Stability of the Developed Genosensor

In order to define the reproducibility of proposed genosensor, the mean intra-assay coefficient of variation coefficient of variation (CV). for 10 and 100 pM of target methylated DNA estimated to be 3.0–2.1% respectively, and the inter-assay was 5.2

and 3.8%. Furthermore, the performance of nanogenosensor in the biological sample was examined by adding two concentrations of target methylated DNA (10, 100, and 1000 pM) to plasma samples. The obtained recovery results are presented in Table 1, showing suitable data with relative standard deviation (RSD) values ranging between 0.63% and 5.25%. The recovery is between 99.84% and 104.3%, that clearly demonstrate the capability of the presented method for detection of methylated DNA in real samples.

The accelerated stability of the modified electrodes was defined. Various SPCEs were prepared under the same procedure as explained in the Method section, stored and assessed in 3 days (data not shown) our prior publication.¹⁶ The response of the nanogenosensor stayed stable within the limits up to 21 h. Then, the developed nanogenosensor showed an average of 22% reduction in electrochemical sensing performance.

Conclusion

In this study, we have developed immuno-DNA electrochemical sensing platform using poly(L-Arg)/RGO composite film and Fe₃O₄/TMC/Au nanocomposite as labeling tags for the rapid, simple, and sensitive detection of methylated biomarker. The fabricated nanogenosensor exhibited good linear range with a low detection limit of 0.01 pM, providing a useful alternative technology to the conventional methodologies.

Moreover, the synergistic influence of RGO and poly(L-Arg) led to a great analytical performance of the sensing platform which can be applied to determine methylated DNA biomarker with suitable results.

Acknowledgments

This research has been supported by Tehran University of Medical Sciences (TUMS), Grant No. 26027.

Conflict of Interest

The authors declare no competing financial interest. ■

References

- Hao X, Luo H, Krawczyk M, Wei W, Wang W, Wang J, et al. DNA methylation markers for diagnosis and prognosis of common cancers. *Proc Natl Acad Sci USA*. 2017;114:7414–7419.
- Paska AV, Hudler P. Aberrant methylation patterns in cancer: a clinical view. *Biochem Med (Zagreb)*. 2015;25:161–176.
- Feinberg AP, Vogelstein B. Hypomethylation distinguishes genes of some human cancers from their normal counterparts. *Nature*. 1983;301:89–92.
- Mikeska T, Craig JM. DNA methylation biomarkers: cancer and beyond. *Genes (Basel)*. 2014;5:821–864.
- Mikeska T, Bock C, Do H, Dobrovic A. DNA methylation biomarkers in cancer: progress towards clinical implementation. *Expert Rev Mol Diagn*. 2012;12:473–487.
- Warton K, Samimi G. Methylation of cell-free circulating DNA in the diagnosis of cancer. *Front Mol Biosci*. 2015;2:13.
- Li Y, Song L, Gong Y, He B. Detection of colorectal cancer by DNA methylation biomarker SEPT9: past, present and future. *Biomark Med*. 2014;8:755–769.
- Song L, Jia J, Peng X, Xiao W, Li Y. The performance of the SEPT9 gene methylation assay and a comparison with other CRC screening tests: a meta-analysis. *Sci Rep*. 2017;7:3032.
- Nian J, Sun X, Ming S, Yan C, Ma Y, Feng Y, et al. Diagnostic accuracy of methylated SEPT9 for blood-based colorectal cancer detection: a systematic review and meta-analysis. *Clin Transl Gastroenterol*. 2017;8:e216.
- Kurdyukov S, Bullock M. DNA methylation analysis: choosing the right method. *Biology (Basel)*. 2016;5. pii: E3.
- Noehammer C, Pulverer W, Hassler MR, Hofner M, Wielscher M, Vierlinger K, et al. Strategies for validation and testing of DNA methylation biomarkers. *Epigenomics*. 2014;6:603–622.
- Syedmoradi L, Esmaili F, Norton ML. Towards DNA methylation detection using biosensors. *Analyst*. 2016;141:5922–5943.
- Taleat Z, Mathwig K, Sudhölter EJR, Rassaei L. Detection strategies for methylated and hypermethylated DNA. *TrAC, Trends Anal Chem*. 2015;66:80–89.
- Krejčova L, Richtera L, Hyněk D, Labuda J, Adam V. Current trends in electrochemical sensing and biosensing of DNA methylation. *Biosens Bioelectron*. 2017;97:384–399.
- Hossain T, Mahmudnabi G, Masud MK, Islam MN, Ooi L, Konstantinov K, et al. Electrochemical biosensing strategies for DNA methylation analysis. *Biosens Bioelectron*. 2017;94:63–73.
- Daneshpour M, Moradi LS, Izadi P, Omidfar K. Femtomolar level detection of RASSF1A tumor suppressor gene methylation by electrochemical nano-genosensor based on Fe₃O₄/TMC/Au nanocomposite and PT-modified electrode. *Biosens Bioelectron*. 2016;77:1095–1103.
- Rahman MM, Li XB, Lopa NS, Ahn SJ, Lee JJ. Electrochemical DNA hybridization sensors based on conducting polymers. *Sensors (Basel)*. 2015;15:3801–3829.
- Liu Z, Forsyth H, Khaper N, Chen A. Sensitive electrochemical detection of nitric oxide based on AuPt and reduced graphene oxide nanocomposites. *Analyst*. 2016;141:4074–4083.
- Li D, Yang XL, Xiao BL, Geng FY, Hong J, Sheibani N, et al. Detection of guanine and adenine using an aminated reduced graphene oxide functional membrane-modified glassy carbon electrode. *Sensors*. 2017;17. pii: E1652.
- Kanyong P, Rawlinson S, Davis J. A voltammetric sensor based on chemically reduced graphene oxide-modified screen-printed carbon electrode for the simultaneous analysis of uric acid, ascorbic acid and dopamine. *Chemosensors*. 2016;4:25.
- Haque AM, Park H, Sung D, Jon S, Choi SY, Kim K. An electrochemically reduced graphene oxide-based electrochemical immunosensing platform for ultrasensitive antigen detection. *Anal Chem*. 2012;84:1871–1878.
- Jian JM, Liu YY, Zhang YL, Guo XS, Cai Q. Fast and sensitive detection of Pb²⁺ in foods using disposable screen-printed electrode modified by reduced graphene oxide. *Sensors (Basel)*. 2013;13:13063–13075.
- Khoshfetrat SM, Mehrgardi MA. Amplified electrochemical genotyping of single-nucleotide polymorphisms using a graphene-gold nanoparticles modified glassy carbon platform. *RSC Advances*. 2015;5:29285–29293.
- Devadas B, Cheemalapati S, Chen S-M, Ali MA, Al-Hemaid FM. Highly sensing graphene oxide/poly-arginine-modified electrode for the simultaneous electrochemical determination of buspirone, isoniazid and pyrazinamide drugs. *Ionics*. 2015;21:547–555.
- Li Y, Feng X, Zhao L, Pu Q. On-surface formation of polyarginine/reduced graphene oxide film and its application in measuring puerarin in healthcare products. *Int. J. Electrochem. Sci*. 2018;13:3948–3957.
- Zhang F, Wang Z, Zhang Y, Zheng Z, Wang C, Du Y, et al. Simultaneous electrochemical determination of uric acid, xanthine and hypoxanthine based on poly (L-arginine)/graphene composite film modified electrode. *Talanta*. 2012;93:320–325.
- Shirazi H, Daneshpour M, Kashanian S, Omidfar K. Synthesis, characterization and *in vitro* biocompatibility study of Au/TMC/Fe₃O₄ nanocomposites as a promising, nontoxic system for biomedical applications. *Beilstein J Nanotechnol*. 2015;6:1677–1689.
- Daneshpour M, Omidfar K, Ghanbarian H. A novel electrochemical nanobiosensor for the ultrasensitive and specific detection of femtomolar-level gastric cancer biomarker miRNA-106a. *Beilstein J Nanotechnol*. 2016;7:2023–2036.
- Daneshpour M, Karimi B, Omidfar K. Simultaneous detection of gastric cancer-involved miR-106a and let-7a through a dual-signal-marked electrochemical nanobiosensor. *Biosens Bioelectron*. 2018;109:197–205.
- Mousavi MF, Amiri M, Noori A, Khoshfetrat SM. A prostate specific antigen immunosensor based on biotinylated-antibody/cyclodextrin inclusion complex: fabrication and electrochemical studies. *Electroanalysis*. 2017;29:2818–2831.
- Omidfar K, Rasaei MJ, Zraee AB, Amir MP, Rahbarzadeh F. Stabilization of penicillinase-hapten conjugate for enzyme immunoassay. *J Immunoassay Immunochem*. 2002;23:385–398.
- Shirazi H, Ahmadi A, Darzianiazizi M, Kashanian S, Kashanian S, Omidfar K. Signal amplification strategy using gold/N-trimethyl chitosan/iron oxide magnetic composite nanoparticles as a tracer tag for high-sensitive electrochemical detection. *IET Nanobiotechnol*. 2016;10:20–27.

This work is licensed under a Creative Commons Attribution-NonCommercial 3.0 Unported License which allows users to read, copy, distribute and make derivative works for non-commercial purposes from the material, as long as the author of the original work is cited properly.